On the Role of the South Atlantic Atmospheric Circulation in Tropical Atlantic Variability

Marcelo Barreiro, [1,2] Alessandra Giannini, [3] Ping Chang, [1] R. Saravanan. [4]

One dominant manifestation of tropical Atlantic variability (TAV) takes place in March-April-May in the form of a strong inter-hemispheric sea surface temperature gradient coupled to a cross-equatorial near surface atmospheric flow. The variability of this circulation pattern affects the position of the intertropical convergence zone and the regional climate in the surrounding areas. In this study, we investigated the effect of the South Atlantic atmospheric variability on this phenomenon. We found that southern summer atmospheric variability (and to a lesser extent winter variability) can play a pre-conditioning role in the onset of inter-hemispheric anomalies in the deep tropics during the following austral fall. It does so by inducing a sea surface temperature anomaly in the southern tropics that initiates local thermodynamic air-sea feedbacks. This remote influence of the Southern Hemisphere on TAV is contrasted with the remote influence of El Niño-Southern Oscillation (ENSO) and the North Atlantic Oscillation (NAO) during austral summer. The results suggest that to fully understand TAV and its predictability it is necessary to consider not only the remote influences from ENSO and NAO, but also the influence from the South Atlantic atmospheric circulation.

1. INTRODUCTION

The coupled variability of an anomalous inter-hemispheric sea-surface temperature (SST) gradient and a cross-equatorial atmospheric circulation that is associated with a displacement of the intertropical convergence zone (ITCZ) during March-April-May (MAM) has long been recognized as one of the

[1] Department of Oceanography, Texas A&M University, College Station, Texas.
[2] Now at Program in Atmospheric and Oceanic Sciences, Princeton University, Princeton, New Jersey.
[3] International Research Institute for Climate Prediction, Columbia University, Palisades, New York.
[4] National Center for Atmospheric Research, Boulder, Colorado.

Ocean-Atmosphere Interaction and Climate Variability
American Geophysical Union Geophysical Monograph

most important components of tropical Atlantic variability (TAV) [e.g., *Hastenrath*, 1985]. This pattern of variability, which we will refer to as the "gradient mode", is known to have a significant impact on rainfall patterns over Northeastern Brazil [e.g., *Hastenrath and Greischar*, 1993]. Understanding and predicting the onset of this phenomenon is one of the central foci of TAV research.

The physical mechanism behind the gradient mode was first outlined by *Hastenrath and Greischar* [1993]: an anomalous cross-equatorial SST gradient generates surface winds from the cooler to the warmer hemisphere through the hydrostatic effect of SST on sea level pressure [*Lindzen and Nigam*, 1987]. The anomalous cross-equatorial winds influence convection by changing the position of moisture convergence. The observed seasonality of this coupling is argued to be a result of the spatially uniform warm climatological SST conditions in austral fall that make the Atlantic ITCZ highly sensitive to small perturbations in the meridional direction [*Chiang et al.*, 2002]. Since the South Atlantic influence is the focus of this work, throughout this paper the seasons refer to those of the Southern Hemisphere (SH), unless explicitly noted.

The genesis and evolution of the gradient mode is shown in Figure 1. This figure is constructed by lag-regressing observed 1000 hPa winds, surface downward heat flux and SST (see section 2) onto an index characterizing the cross-equatorial SST gradient during MAM. The gradient index used here, GI, is constructed as the average of the SST anomaly over $4°$-$14°$S,$40°$-$10°$W minus the average of the SST anomaly over $4°$-$14°$N,$60°$-$30°$W during MAM (hereafter MAM1). The seasons preceding MAM1 are denoted as JJA0, SON0 and DJF1 for June-July-August, September-October-November of the previous year, and December-January-February of the same year. The evolution shows that large cross-equatorial gradients are preceded by SST anomalies on both sides of the equator in the previous seasons. The maps suggest that the initial subtropical SST anomaly is generated through wind-induced changes in the surface heat fluxes during JJA0, SON0 and DJF1 [*Wagner*, 1996]. The magnitude of the tropical SST anomaly in the SH tends to be larger than that in the Northern Hemisphere (NH) up to DJF1. Also, in the SH the SST anomaly does not grow as much as in the NH from DJF1 to MAM1. This suggests that in the NH atmospheric variability during boreal winter plays the most important role in producing the northern SST anomaly that forms the gradient, while in the SH atmospheric variability during several seasons plays a role. In MAM1 surface winds are concentrated in the deep tropics, flowing from the cooler to the warmer hemisphere and inducing changes in the surface heat fluxes that strengthen the already existing cross-equatorial SST gradient. This in

Figure 1

turn strengthens the winds, closing the loop of a positive feedback. This feedback mechanism was formally put forth by *Chang et al.* [1997] to explain the gradient mode, and is also known as Wind-Evaporation-SST (WES) feedback [*Xie and Philander*, 1994]. Evidence of local air-sea feedbacks in the tropical Atlantic comes from observational [*Chiang et al.*, 2002] and modeling studies [*Carton et al.*, 1996; *Chang et al.*, 1997, 2000; *Xie*, 1999]. The existence of this feedback may be fundamental for extending seasonal prediction beyond persistence.

From Figure 1, it is clear that identifying and understanding the sources of the SST anomalies associated with the gradient mode are important aspects of TAV research. Among the known sources of SST anomalies in the tropical North Atlantic are ENSO [e.g., *Curtis and Hastenrath*, 1995; *Enfield and Mayer*, 1997; *Saravanan and Chang*, 2000], and the NAO [e.g., *Marshall et al.*, 2001]. The impact of ENSO on TAV is believed to be as follows: During warm ENSO events diabatic heating anomalies in the tropical Pacific cause the northeasterly trades in the tropical Atlantic to weaken during summer, which coincides with the mature phase of ENSO. This reduces the evaporational cooling, and generates a positive SST anomaly in the northern tropics. *Chiang et al.* [2002] and *Giannini et al.* [2001] show that ENSO generally tends to aid the development of an SST gradient in the following fall. However, the anomalous gradient can also form in the absence of ENSO [*Chiang et al.*, 2002]. This latter result underlies the importance of local feedbacks. In fact, a recent study by *Giannini et al.* [2004] suggests that the local feedbacks can interfere with the remote influence of ENSO.

The NAO is the dominant mode of internal atmospheric variability during boreal winter. The oceanic response to the NAO forcing consists of a tripole pattern in SST anomalies, extending from the high latitudes of the North Atlantic to the northern tropics with decreasing amplitude [*Visbeck et al.*, 1998]. Observational and modeling studies show that during a strong NAO year northeasterly trade winds strengthen and generate a negative SST anomaly in the tropical North Atlantic via changes in latent heat flux. The resulting SST anomaly has its largest amplitude near the African coast north of 10°N [*Chang et al.*, 2001; *Czaja et al.*, 2002]. Studies show that NAO plays an important role in initiating local air-sea feedbacks in the deep tropical Atlantic region [*Halliwell*, 1997; *Xie and Tanimoto*, 1998; *Chang et al.*, 2001]. However, *Wu and Liu* [2002] found that although NAO can enhance variability in the tropical North Atlantic, its occurrence is not a requirement for the development of the gradient mode.

Until now, the origin of SST anomalies in the southern tropical Atlantic has been largely ignored, probably due to the lack of reliable observational data. The origin of the south-

ern SST anomaly may be tied to the northern SST anomaly through the WES feedback. Several authors have argued, however, that the two lobes of the gradient in MAM1 seen in Figure 1 are largely independent and that a dipole does not exist as a physical mode, but is an artifact of construction [e.g., *Enfield et al.* 1999; *Dommenget and Latif*, 2000; *Czaja et al.*, 2002]. This, however, does not exclude the existence of the WES mechanism which may act to strengthen an already existing cross-equatorial gradient.

In a recent observational study, *Sterl and Hazeleger* [2003] found that SST anomalies in the South Atlantic are generated mainly through atmosphere-induced latent heat fluxes and wind-induced mixed layer deepening, and damped by latent heat fluxes. Their results and those of *Venegas et al.* [1997] agree on that the leading mode of observed coupled variability in the basin consists of a weakened/strengthened subtropical anticyclone forcing the ocean, independent of ENSO. *Venegas et al.* [1997] further found that this coupling is strongest during summer, and argued this is due to a link between the SH atmosphere and climate fluctuations in the NH, such as the NAO. On the other hand, the South Atlantic anticyclone is most energetic during winter [*Satyamurty et al.*, 1998], when it reaches its westernmost and northernmost position [*Hastenrath*, 1985]. Therefore, variability of the subtropical high during this season is likely to have an influence on TAV.

In this work, we take a further look at the atmospheric variability in the South Atlantic and explore its influence on TAV. We show that TAV is influenced not only by ENSO and the NAO, but also by atmospheric variability in the South Atlantic during austral winter and summer. Moreover, our results suggest that local air-sea feedbacks play an important role in maintaining the tropical SST anomaly and strengthening the cross-equatorial gradient.

The paper is organized as follows. In the next section we study the evolution of the SST anomaly generated by the leading mode of winter atmospheric variability in the South Atlantic. A mechanism through which this atmospheric pattern can affect the development of the gradient mode in the following fall is proposed and tested using a model. Section 3 investigates the observed evolution of the SST anomaly generated by the leading mode of atmospheric variability in SH summer, and its influence on TAV. In section 4 we compare the relative influence of ENSO, NAO and the South Atlantic atmospheric circulation on the development of the gradient mode. The last section summarizes the main results.

2. SOUTH ATLANTIC WINTER ATMOSPHERIC VARIABILITY AS EXTERNAL FORCING OF TAV

Figure 1 suggests that atmospheric variability in SH winter and summer plays a role in forcing the SST anomaly in the southern tropics that later becomes a part of the cross-equatorial gradient. This SST anomaly is created in the subtropics and afterward strengthens in the equatorial region, particularly from DJF1 to MAM1. In this paper we define winter to go from June to September (JJAS), and summer from November to February (NDJF). This section considers the winter, while section 3 is devoted to the influence of the summer season.

We use the reconstructed SST data set of *Smith et al.* [1996]. We also use 1000 hPa winds, sea level pressure and surface heat fluxes from the NCEP/NCAR Reanalysis [*Kalnay et al.*, 1996]. All data sets have a spatial resolution of approximately 2.8° (T42) and span from January 1950 to December 1994. It should be noted that the quality of the data especially in the SH is more reliable after the introduction of satellites in the 1980s. To diagnose the atmospheric response to oceanic conditions during MAM we also consider the Xie-Arkin precipitation data set [*Xie and Arkin*, 1997], which is available since 1979 on a T42 grid. The regression plots in Figure 4 below were constructed for the common period, 1979 to 1994. Significance levels throughout this study are calculated according to a two-sided Student's t-test, assuming no year-to-year correlation.

2.1. Observed Evolution

We calculated the Empirical Orthogonal Functions (EOFs) of (detrended) 1000 hPa wind speed during JJAS within 60°W-20°E,40°-0°S, the region that contains the seasonal mean position of the anticyclone. The leading EOF (hereafter winter-EOF) explains 31% of the total variance and is well separated from the second one. A simultaneous regression of sea level pressure shows that the winter-EOF represents a weakening/strengthening of the subtropical high in the South Atlantic with weak correlations outside this basin except in the Southern Indian Ocean (Figure 2a). This is consistent with *Sterl and Hazeleger* [2003]. The principal component (PC) associated with the winter-EOF (hereafter P1JJAS) presents mainly interannual time scales (Figure 2b). This PC has no significant correlations (above the 95% level) with ENSO or with equatorial Atlantic SST during winter. In this study we use Nino3.4 (the average of SST anomalies in 120°-170°W,5°S-5°N) to characterize ENSO, and ATL3 (the average of SST anomalies in 20°W-0°E,3°S-3°N) to characterize equatorial Atlantic SST [*Zebiak*, 1993]. The P1JJAS index has no significant correlation with the GI in

Figure 2

the next austral fall. However, it is significantly correlated at $r = 0.4$ with the southern tropical index used to construct GI. Thus, it appears that the winter atmospheric variability can influence southern tropical SST and thus TAV three seasons in advance. To investigate this issue, we regress 1000 hPa winds, surface heat flux and SST on P1JJAS for the seasons JJA0, SON0, DJF1 and MAM1 ("0" indicates the year in which the EOF is calculated). This is shown in Figure 3. The maps show, that during winter, cyclonic wind anomalies force the ocean through changes in the heat fluxes in the subtropical South Atlantic. A decomposition into the different heat flux components indicates that latent heat flux changes dominate. The ocean responds with a 2- to 3- month lag in SST change. The subtropical SST anomaly tends to persist into the next season (DJF1) with a noticeable northwestward shift. During this season the SST gradient created by the existence of the southern SST anomaly induces cross-equatorial northerly winds which tend to cool the northern deep tropics and warm the southern tropics through changes in the latent heat flux. This suggests the possibility of a WES feedback. Changes in the solar radiation tend to oppose the creation of SST anomalies in the northern tropics, but help maintaining the SST anomaly in the southern tropics. As a result, the SST anomaly south of the equator persists into MAM1, when it is accompanied by cross-equatorial winds. Subtropical wind anomalies are also present south of the maximum SST anomaly. Since Figure 3 is constructed by regressing onto an index characterizing the atmosphere 3 seasons before, these subtropical winds can only be interpreted as a response to the SST anomaly unless they are a statistical artifact and occur by chance. During MAM1 the tropical atmosphere is so sensitive to ocean conditions that even the small SST gradient tends to shift the ITCZ toward the SH (Figure 4a).

Figure 3

Figure 4

The persistence of the SST anomaly between $5°$S-$20°$S from the coast of Brazil to $20°$W may also be attributed to a relatively deep mixed layer in the region. The annual mean mixed layer depth is larger than 40m, while in the western tropical North Atlantic the mixed layer depth is less than 30m (see Figure 1 of *Saravanan and Chang* [this volume]).

2.2. Simulated Evolution Using an Atmospheric General Circulation Model Coupled to a Slab Ocean

In the previous section we found that the evolution of the SST anomaly in the subtropical South Atlantic is mainly governed by surface heat flux anomalies. This result is consistent with *Sterl and Hazeleger* [2003], although other processes like mixed layer deepening or Ekman pumping may also play a role. In this section we use an atmospheric general circulation model coupled to a slab ocean to show that the main char-

acteristics of the observed evolution of Figure 3 can indeed be ascribed to thermodynamic ocean-atmosphere coupling. We use the Community Climate Model 3.6 (CCM3) developed at the National Center for Atmospheric Research coupled to a slab ocean with an annual mean mixed layer depth. The model has been shown to represent TAV realistically [*Saravanan and Chang*, 1999], and is described by *Saravanan and Chang* [this volume]. We use a 100 year control run in which CCM3 is coupled everywhere to the slab ocean (referred as experiment MIXL in *Saravanan and Chang* [this volume]). This setup excludes any dynamical ocean-atmosphere interaction, and thus ENSO and the Atlantic zonal mode [*Zebiak*, 1993] are not present. To assure the correct simulation of the annual cycle of SST the slab ocean uses a Q-flux correction that accounts for the missing climatological ocean dynamics in the model. For a detailed model description we refer the readers to the above referenced article.

We applied the same analysis of Figures 2 and 3 to the model output. The leading EOF of 1000 hPa wind speed in the South Atlantic during JJAS explains 32% of the total variance. The anomalous pattern of sea level pressure is similar to the observed one (not shown). It represents a weakening/strengthening of the South Atlantic anticyclone, and is correlated with pressure anomalies in the South Indian Ocean. It is also significantly correlated with pressure anomalies over the Pacific Ocean at about $160°$E,$20°$N that is not found in observations. This may be related to the absence of ENSO in the model.

Figure 5 shows the simulated evolution of 1000 hPa winds, surface heat flux and SST by regressing these fields onto the PC of the leading winter EOF. Clearly, the simulated evolution is similar to the observed one. During winter cyclonic winds associated with a weakened subtropical high generate a positive downward heat flux anomaly in the southern subtropics, producing the largest response 2 or 3 months later. In DJF1 the SST anomaly is damped in the subtropics, but maintained and even strengthened in the western deep tropics, presumably through a positive feedback involving surface winds, heat flux and SST. This results in a shift of the position of maximum SST anomaly toward the equator. The cross-equatorial southward surface flow induces a negative heat flux in the northern deep tropics that tends to cool the region. As in observations, changes in latent heat flux are opposed by the negative feedback provided by solar radiation changes due to changes in cloud cover as the ITCZ shifts toward warm waters. This result is also consistent with the observational work of *Tanimoto and Xie* [2002]. The cross-equatorial SST gradient and accompanied surface winds are strongest in MAM1. Note that simulations do not show significant subtropical wind anomalies during MAM1, as observations do (see Figure 3).

Figure 5

The fact that we are able to reproduce the main characteristics of the observed evolution supports the idea that thermodynamic interaction dominates ocean-atmosphere coupling, in general agreement with *Sterl and Hazeleger* [2003]. Here, however, we find evidence for local air-sea feedbacks in the deep tropics. Results also support that winter atmospheric variability can influence the development of the gradient mode.

It is worth pointing out that there are some important differences between simulated and observed fields. First, the simulated wind anomaly in winter is shifted about 10° west compared to observations, hence the maximum in SST anomaly is also shifted to the west. Second, the SST variance explained by the atmospheric forcing is larger in the simulation because SST anomalies in the model ocean only occur through surface heat fluxes, while in the real ocean other dynamical processes are present. The exaggerated SST response in the model may also be attributed to the use of an annual mean mixed layer depth which underestimates its value during winter (see Figure 1 of *Saravanan and Chang* [this volume]). This effect, together with the absence of ocean processes that tend to damp the SST anomaly in the equatorial region [*Chang et al.*, 2001], overestimates the importance of the local feedback and exaggerates the simulated cross-equatorial SST gradient and winds in the fall.

3. SOUTH ATLANTIC SUMMER ATMOSPHERIC VARIABILITY AS EXTERNAL FORCING OF TAV

We next consider the summer season. The leading EOF of 1000 hPa wind speed during NDJF in the South Atlantic explains 28% of the total variance and is well separated from the second one. We will refer to it as the summer-EOF and to its PC as P1NDJF. The regression of sea level pressure shows a weakened/strengthened anticyclone in the South Atlantic (Figure 6a). The regression map does not show any significant correlation with NH anomalies, except maybe over North America. On the other hand, the variability of the subtropical high seems to be part of a global pattern resembling the southern annular mode [*Thompson and Wallace*, 2000]. It also presents a wavenumber 4 structure with maximum amplitude at about 45°S. Recently, *Fauchereau et al.* [2003] reported a similar wavenumber 4 pattern of sea level pressure variability in the SH. They found that during summer the surface winds associated with this structure force the South Atlantic and South Indian Ocean simultaneously through changes in the latent heat flux. Their analysis indicates that the structure is not significantly correlated with the annular mode. Here, we calculated an index for the annular mode as the first principal component of sea level pressure

Figure 6

south of $20°$S. This time series is correlated with P1NDJF at $r = 0.33$ (just above the 95% significance level).

The summer-EOF shows longer time scales than the winter-EOF (Figure 6b), and P1NDJF is not correlated to ENSO or the NAO. It is, however, correlated with GI at $r = 0.46$, indicating that this mode influences TAV. Figure 7 shows the regression of 1000 hPa winds, surface heat flux and SST onto P1NDJF for DJF1 and MAM1. As in the winter case, there is an eddy-like circulation over the subtropical Atlantic which induces changes in the surface heat fluxes, primarily latent heat. During summer, however, the ocean responds faster and the maximum SST anomaly occurs within the season. The initial SST anomaly is created south of $10°$S, but in MAM1 it has reached the equatorial region. This is a consequence of the response of surface winds to the southern SST anomaly, and the interplay between heat flux, SST and winds -a characteristic of the WES feedback: The cross-equatorial gradient forces northerly winds that tend to cool the SST in the northern tropics through changes in latent heat. At the same time weakened southerly trades tend to induce positive heat flux anomalies in the southern deep tropics that maintain the southern SST anomaly and strengthen the SST gradient. On the other hand, in the southern subtropics the SST anomaly appears to be damped. It is interesting to note that *Czaja et al.* [2002] find evidence of WES feedback in the deep northern tropics when the tropical North Atlantic is forced by anomalous winds during boreal winter.

Figure 7

Thus, the SST anomalies created in summer follow a similar evolution as the anomalies created during winter. In the summer case, however, the SST anomaly in MAM1 is larger because it was created just one season before. This generates a larger atmospheric response, as can be seen in the regression of rainfall onto P1NDJF from 1979 to 1994 (Figure 4b). Clearly, rainfall anomalies are larger than in the winter case (Figure 4a), and are of similar magnitude as those created by the cross-equatorial gradient of Figure 1 (Figure 4c).

Note that the SST anomaly in the southern lobe of the dipole in MAM1 of Figure 1 can be explained to first order by considering the SST anomaly generated by summer atmospheric variability. The SST anomaly generated by winter atmospheric variability plays a secondary role, and is most important between 0 and $10°$S.

One interesting feature is that the summer PC, P1NDJF, is marginally correlated at the 95% level with the winter PC, P1JJAS. Since the atmosphere does not have a long memory, this suggests that the SST anomaly created by winter atmospheric variability forces an atmospheric response in the following summer, and the summer-EOF has a small contribution of this signal. Modeling studies have suggested the existence of an SST-forced response in this region dur-

ing summer [e.g., *Barreiro et al.*, 2002]. We repeated the calculation of the summer-EOF after linearly removing the contribution of the winter-EOF to the 1000 hPa wind speed anomaly. The new leading EOF correlates at $r = 0.95$ with P1NDJF. Also, the evolution of SST, surface winds and heat flux does not change significantly from that of Figure 7. Thus, in this work we consider the summer-EOF to mainly represent internal atmospheric variability.

4. RELATIONSHIP BETWEEN THE CROSS-EQUATORIAL GRADIENT AND ATMOSPHERIC VARIABILITY IN BOTH HEMISPHERES

According to the results of the previous sections, to first order the SST anomaly in the tropical North Atlantic is independent of the SST in the tropical South Atlantic. Nevertheless, an SST anomaly generated in the southern tropics tends to induce an SST anomaly of opposite sign in the northern tropics through changes in the surface heat fluxes, suggesting the existence of the WES feedback.

To further look into this issue we classify the cross-equatorial gradient index as a function of indices of southern and northern atmospheric variability. The largest gradients are expected when the atmospheric anomalies on both sides of the equator are such that they tend to generate SST anomalies of opposite sign. If hemispheres are independent, the existence of an SST anomaly in one hemisphere would not affect the development of the SST anomaly in the other hemisphere. We use GI to characterize the cross-equatorial gradient in MAM. Atmospheric variability in the NH is characterized by the influences of ENSO and the NAO. To characterize ENSO we consider the Nino3.4 index during December-January (Nino34DJ), which is correlated with GI at $r = -0.5$. To characterize the NAO we consider the time series calculated as the difference of normalized sea level pressure between Lisbon, Portugal, and Reykjavik, Iceland, from December to March. The time series was obtained from the web site http://www.cgd.ucar.edu/∼hurrell/nao.stat.winter.html, and was detrended by removing the least squares linear fit prior to the analysis. This NAO index is not significantly correlated with GI. We use P1JJAS and P1NDJF to characterize winter and summer atmospheric variability in the South Atlantic, respectively. These indices are not significantly correlated to Nino34DJ or the NAO index.

We investigate the relationship among the atmospheric indices and the sign and intensity of the gradient in MAM by constructing scatter plots (Plate 1). In these plots the color of the marker indicates the sign and intensity of GI, while different pair of indices are used as coordinate axes. Since the atmospheric indices are not correlated the distribution

Plate 1

of points tends to be circular. The scatter plots show how different combinations of atmospheric indices determine the sign and magnitude of GI.

We first consider the summer-EOF (P1NDJF) and the NAO (Plate 1a). The plot clearly shows that the sign of the gradient is mainly given by the sign of the summer-EOF. Most positive cross-equatorial gradients correspond to a situation when the summer-EOF is positive, that is, when the South Atlantic atmospheric variability induces a positive SST anomaly in the southern subtropics. The NAO index does not have an appreciable influence on GI, consistent with the non-significant correlation between these two indices. This is in part due to our choice of GI. The NAO tends to influence SST north of 10°N [e.g., *Ruiz-Barradas et al.*, 2000, 2003; *Czaja et al.*, 2002], and the induced SST anomaly has maximum amplitude near the African coast. The GI was constructed using SST anomalies in the western tropical Atlantic. This is the region of maximum seasonal precipitation, where SST anomalies can more easily induce a response, and away from the region of maximum NAO influence. Note that the intensity of the GI is not clearly related to P1NDJF. For positive GI there is a tendency for large gradients to occur when P1NDJF is large (close to 1), but that is not true for negative GI. An analogous scatter plot using NAO and the winter-EOF does not show a clear relationship between the indices and GI (Plate 1b). There is a tendency, however, for positive gradients to occur when both NAO and P1JJAS are positive (upper right quadrant), that is, when the NAO (SH winter) cools (warms) the northern (southern) tropics.

We now turn to the relationship between GI, ENSO and the SH indices. Plate 1c shows the scatter plot using Nino34DJ and P1NDJF (summer-EOF) indices. Note that in the plot we changed the sign of Nino3.4, so that El Niño events correspond to negative values. We define ENSO events as those when Nino34DJ is larger than 0.75K. This classification leads to the following El Niño events: 1958, 1964, 1966, 1969, 1970, 1973, 1983, 1987, 1988 and 1992, and the following La Niña events: 1951, 1955, 1956, 1965, 1971, 1972, 1974, 1976, 1985 and 1989 (years refer to the January month). In Plates 1c,d El Niño events are marked with a "o", while La Niña events are marked with a "+". El Niño (La Niña) events tend to warm (cool) the tropical North Atlantic. Thus, El Niño (La Niña) events are expected to induce negative (positive) GI values during MAM. From Plate 1c it is clear that the cross-equatorial gradient is strongest when (-1)*Nino34DJ and the summer-EOF (P1NDJF) indices are both of the same sign, that is, GI is largest when atmospheric anomalies on both sides of the equator induce SST anomalies of opposite sign (upper right and lower left quadrants). The largest positive values of GI occur when both P1NDJF and (-1)*Nino34DJ are large. On the other hand, the largest neg-

ative values of GI occur for small negative values of P1NDJF, but for large (negative) values of (-1)*Nino34DJ. This suggests that the amplitude of the large negative cross-equatorial gradients is set up mainly by the remote signal from El Niño events.

When the southern atmosphere in summer generates an SST anomaly of the same sign as the SST anomaly to be created by ENSO in the northern tropics (lower right and upper left quadrants in Plate 1c), the resulting gradient in MAM is usually weak. There are 8 ENSO events in this category: El Niño years 1964, 1969, 1973 and 1988, and La Niña years 1951, 1955, 1956 and 1976 (see Plate 1c). Seven of these years have GI values close to neutral or of opposite sign as those expected from ENSO forcing acting alone. Moreover, during most of these years the sign of the cross-equatorial gradient is given by the sign of P1NDJF. To investigate if the pre-existing southern SST anomaly influenced the northern tropics, we look at the sign of the northern index used to construct GI. We found that during El Niño of 1988 and La Niña of 1955 and 1976 the sign is as expected from ENSO forcing. However, during the ENSO events of 1951, 1956, 1964 and 1973 the northern tropics have (weak) SST anomalies of the opposite sign from the expected ENSO signal. This may be explained by the NAO forcing acting against the ENSO forcing in the northern tropics. However, only 1973 is a strong NAO year (> 0.5 standard deviation) that acts against the ENSO forcing. Thus, this suggests that during these years the hemispheres were not independent, but that local feedbacks initiated by the southern tropical SST influenced the northern tropics and worked against the remote ENSO forcing.

These results agree with those of *Giannini et al.* [2004] and *Barreiro et al.* [2004], who suggest that the WES feedback and the remote influence of ENSO can interfere constructively or destructively. Constructive interference occurs when both processes tend to create a cross-equatorial gradient of the same sign. Destructive interference occurs when the WES feedback and the remote ENSO signal act against each other. Our findings suggest that during 1951, 1956, 1964 and 1973 the WES feedback initiated by the SH summer atmospheric variability worked against the remote ENSO forcing, changing the gradient to that expected from ENSO acting alone. During other years the local feedback can be overpowered by ENSO, but may still reduce the SST anomaly in the northern tropics.

Year 1969 is the only case in which a relatively large negative gradient occurs when the South Atlantic summer atmospheric circulation induces a positive SST anomaly in the southern tropics. During this year the remote forcing from El Niño superposed with the weakest NAO on record (see Plate 1a). Thus, the northern tropics developed a large

positive SST anomaly that overpowered the local feedbacks and changed the sign of the GI.

These findings show that the summer-EOF pre-conditions the development of the gradient mode in MAM by initiating local air-sea feedbacks, which can interfere constructively or destructively with the remote ENSO signal. Consequently, although to first order the hemispheres are independent, they tend to be connected during the time when the local WES feedback is important. Plate 1d shows the case using Nino34DJ and P1JJAS. As before, ENSO is a good predictor of GI, and the strongest cross-equatorial gradients tend to occur when the indices have the same sign. The pre-conditioning of the gradient from the winter-EOF is, however, less clear than that from the summer-EOF probably because the induced summer SST anomaly is weaker. Thus, the results from this section show that Nino34DJ and P1NDJF are the best predictors for the GI.

5. SUMMARY

We presented an exploratory study of the influence of the South Atlantic atmospheric circulation on TAV. We first calculated the leading patterns of austral winter and summer atmospheric variability in the South Atlantic. They consist of a weakening/strengthening of the anticyclone forcing the ocean below, consistent with the literature [*Venegas et al.*, 1997; *Sterl and Hazeleger*, 2003]. Using regression analysis, we next studied the evolution of the SST anomalies generated, and their possible role in the development of the gradient mode. The relative importance of South Atlantic atmospheric variability in TAV, and specifically in determining the sign of the cross-equatorial SST gradient during fall, is addressed by comparing its role versus that of ENSO and the NAO. The main results are the following (seasons refer to those of the SH):

- Winter atmospheric variability in the South Atlantic induces an SST anomaly that tends to persist until the next fall. Observational and modeling studies suggest that ocean and atmosphere interact mainly through surface heat fluxes. This is consistent with the literature, although other processes like wind-induced mixed layer deepening may also play a role in generating the initial SST anomaly [*Sterl and Hazeleger*, 2003]. The following scenario is proposed: In winter the weakened southeasterly trade winds remove less heat from the ocean, generating a warm SST anomaly. In the following seasons the SST anomaly is damped in the subtropics, but not in the western deep tropics. The existing SST gradient induces southward cross-equatorial winds during summer, which tend to cool the SST in the northern deep tropics and maintain the SST anomaly in the south through the WES feedback mechanism. The weak SST gradient that

persists until MAM favors a southward shift of the ITCZ. Although the influence of winter atmospheric variability on TAV is weaker than that of summer, it may be important for enhancing seasonal prediction. More research on this subject is clearly needed. But, if this conjecture turns out to be true then knowledge of the atmospheric conditions during austral winter would allow prediction of the SST anomaly, and thus of the location of the ITCZ, more than two seasons in advance.

- Summer atmospheric variability in the South Atlantic also forces the ocean below through changes in the latent heat fluxes, in agreement with *Fauchereau et al.* [2003]. In this season the ocean responds faster than in winter, perhaps due to a shallower mixed layer depth. The SST anomaly is created south of 10°S, but moves northwestward by means of the WES feedback mechanism. As a result, the SST anomaly induces a strong atmospheric response in the austral fall, shifting the ITCZ toward anomalously warm waters.

- Summer atmospheric variability (and to a lesser extent winter variability) in the South Atlantic pre-conditions the development of strong cross-equatorial gradients during the next fall. It does so by generating an SST anomaly in the southern tropics during summer, which initiates the WES feedback in the deep tropics. This mechanism will in turn tend to strengthen the cross-equatorial gradient. When the ENSO remote influence creates an SST anomaly of opposite sign as that already present in the southern tropics the resulting gradient in MAM is strongest. When the ENSO forced signal is of the same sign the outcome will depend on the relative strengths of ENSO and the WES feedback. An interesting result, also found in *Giannini et al.* [2004], is that the constructive/destructive interference seems to depend only on the southern tropical SST in DJF, and not on the cross-equatorial SST gradient on that season. A possibility is that ENSO and NAO forcings are so strong that they can wipe out any SST anomaly that was present in the northern tropics during DJF. Thus, to first order, the cross-equatorial gradient will only be pre-conditioned by the southern tropics. Further study is needed to address this issue.

Results show that atmospheric circulation in the South Atlantic is capable of initiating local air-sea feedbacks in the tropics, and affecting the development of the gradient mode, as previously found for the NH atmosphere [e.g., *Xie and Tanimoto*, 1998]. These findings suggest that to fully understand TAV it is necessary to consider not only the remote influence of ENSO and the NAO, but also of the southern atmospheric circulation during winter and summer. These remote phenomena, together with the local feedbacks, control the evolution of SST in the tropical Atlantic. The existence of so many players involved in TAV makes prediction

of tropical Atlantic climate very challenging, and calls for sustained observations in the region.

Acknowledgments. The authors would like to thank two anonymous reviewers for their constructive criticism that greatly improved the original manuscript. M.B. was supported by NASA Headquarters under the Earth System Science Fellowship Grant NGT5-30417. This study is supported by the NOAA and NSF grants: NA16GP1572 and ATM-99007625. P.C. also acknowledges the support from the National Natural Sciences Foundation of China (NSFC) through Grant 40128003.

REFERENCES

Barreiro, M., P. Chang, and R. Saravanan, Variability of the South Atlantic Convergence Zone simulated by an atmospheric general circulation model, *J. Clim.*, *15*, 745-763, 2002.

Barreiro, M., P. Chang, L. Ji, R. Saravanan, and A. Giannini, Dynamical elements of predicting boreal spring tropical Atlantic sea-surface temperatures, *Dyn. Atmos. Oceans*, submitted, 2004.

Carton, J. A., X. Cao, B. Giese, and A. M. Da Silva, Decadal and interannual SST variability in the tropical Atlantic Ocean, *J. Phys. Oceanogr.*, *26*, 1165-1175, 1996.

Chang, P., L. Ji, and H. Li, A decadal climate variation in the tropical Atlantic ocean from thermodynamic air-sea interactions, *Nature*, *385*, 516-518, 1997.

Chang, P., R. Saravanan, L. Ji, and G. C. Hegerl, The effect of local sea surface temperatures on atmospheric circulation over the tropical Atlantic sector, *J. Clim.*, *13*, 2195-2216, 2000.

Chang, P., L. Ji, and R. Saravanan, A hybrid coupled model study of tropical Atlantic variability, *J. Clim.*, *14*, 361-390, 2001.

Chiang, J. C. H., Y. Kushnir, and A. Giannini, Deconstructing Atlantic ITCZ variability: Influence of the local cross-equatorial SST gradient, and remote forcing from the eastern equatorial Pacific, *J. Geophys. Res.*, *107*(D1), 1-19, 2002.

Curtis, S., and S. Hastenrath, Forcing of anomalous sea surface temperature evolution in the tropical Atlantic during Pacific warm events, *J. Geophys. Res.*, *100*, 15,835-15,847, 1995.

Czaja, A., P. van der Vaart, and J. Marshall, A diagnostic study of the role of remote forcing in tropical Atlantic variability, *J. Clim.*, *15*, 3280-3290, 2002.

Dommenget, D., and M. Latif, Interannual to decadal variability in the tropical Atlantic, *J. Clim.*, *13*, 777–792, 2000.

Enfield, D. B., and D. A. Mayer, Tropical Atlantic sea surface temperature variability and its relation to El Niño-Southern Oscillation, *J. Geophys. Res.*, *102*, 929-945, 1997.

Enfield, D. B., A. M. Mestas-Nunez, D. A. Mayer, and L. Cid-Serrano, How ubiquitous is the dipole relationship in tropical Atlantic sea surface temperatures?, *J. Geophys. Res.*, *104*, 7841-7848, 1999.

Fauchereau, N., S. Trzaska, Y. Richard, P. Roucou, and P. Chamberlin, Sea surface temperature co-variability in the Southern Atlantic and Indian Oceans and its connection with the atmospheric circulation in the southern hemisphere, *Int. J. Climatol.*, *23*, 663-677, 2003.

Giannini, A., J. C. H. Chiang, M. Cane, Y. Kushnir, and R. Seager, The ENSO teleconnection to the tropical Atlantic Ocean: contributions of the remote and local SSTs to rainfall variability in the tropical Americas, *J. Clim.*, *14*, 4530-4544, 2001.

Giannini, A., R. Saravanan, and P. Chang, The preconditioning role of tropical Atlantic variability in the development of the ENSO teleconnection: Implications for the prediction of Nordeste rainfall, *Clim. Dyn.*, submitted, 2004.

Halliwell Jr., G. R. H., Decadal and multidecadal North Atlantic SST anomalies driven by standing and propagating basin-scale atmospheric anomalies, *J. Clim.*, *10*, 2405-2411, 1997.

Hastenrath, S., *Climate and circulation of the tropics*, 455 pp., D. Reidel, 1985.

Hastenrath, S., and L. Greischar, Circulation mechanisms related to northeast Brazil rainfall anomalies, *J. Geophys. Res.*, *98*, 5093–5102, 1993.

Kalnay, E., et al., The NCEP/NCAR 40-year reanalysis project, *Bull. Am. Meteorol. Soc.*, *77*, 437-471, 1996.

Lindzen, R. S., and S. Nigam, On the role of sea surface temperature gradients in forcing low level winds and convergence in the tropics, *J. Atmos. Sci.*, *44*, 2418-2436, 1987.

Marshall, J., Y. Kushnir, D. Battisti, P. Chang, A. Czaja, R. Dickson, J. Hurrel, M. McCartney, R. Saravanan, M. Visbeck, North Atlantic climate variability: Phenomena, impacts and mechanisms, *Int. J. Climatol.*, *21*, 1863-1898, 2001.

Ruiz-Barradas, A., J. A. Carton, and S. Nigam, Structure of interannual-to-decadal climate variability in the tropical Atlantic sector, *J. Clim.*, *13*, 3285-3297, 2000.

Ruiz-Barradas, A., J. A. Carton, and S. Nigam, Role of the atmosphere in climate variability of the tropical Atlantic, *J. Clim.*, *12*, 2052-2065, 2003.

Saravanan R., and P. Chang, Oceanic mixed layer feedback and tropical Atlantic variability, *Geophys. Res. Lett.*, *26*, 3629-3633, 1999.

Saravanan R., and P. Chang, Interaction between tropical Atlantic variability and El Niño-Southern Oscillation, *J. Clim.*, *13*, 2177-2194, 2000.

Saravanan, R., and P. Chang, Thermodynamic coupling and predictability of tropical sea surface temperature, this volume.

Satyamurty, P., C. A. Nobre, and P. L. Silva Dias, South America, in *Meteorology of the Southern Hemisphere*, D. J. Karoly and D. G. Vincent, Eds., Meteorol. Monogr., No. 49, pp. 119-139, Am. Meteorol. Soc., 1998.

Smith, T. M., R. W. Reynolds, R. E. Livezey, and D. C. Stokes, Reconstruction of historical sea surface temperatures using empirical orthogonal functions, *J. Clim.*, *9*, 1403-1420, 1996.

Sterl, A., and W. Hazeleger, Coupled variability and air-sea interaction in the south Atlantic Ocean, *Clim. Dyn.*, *21* , 559-571, 2003.

Tanimoto, Y., and S.-P. Xie, Inter-hemispheric decadal variations in SST, surface winds and cloud cover over the Atlantic Ocean, *J. Meteorol. Soc. Jpn.*, *80*, 1199-1219, 2002.

Thompson, D. W. J., and J. M. Wallace, Annular modes in the extratropical circulation. Part I: Month-to-month variability, *J. Clim.*, *13*, 1000-1016, 2000.

Venegas, S. A., L. A. Mysak, and D. N. Straub, Atmosphere-ocean coupled variability in the south Atlantic, *J. Clim.*, *10*, 2904-2920, 1997.

Visbeck, M., H. Cullen, G. Krahmann, and N. Naik, An ocean model's response to North Atlantic Oscillation-like wind forcing, *Geophys. Res. Lett.*, *25*, 4521-4524, 1998.

Wagner R. G., Mechanisms controlling variability of the interhemispheric sea surface temperature gradient in the Tropical Atlantic, *J. Clim.*, *9*, 2010-2019, 1996.

Wu, L., and Z. Liu, Is tropical Atlantic variability driven by the North Atlantic Oscillation?, *Geophys. Res. Let.*, *13*, doi: 10.1029/2002GL014939, 2002.

Xie, P., and P. A. Arkin, Global precipitation: A 17-year monthly analysis based on gauge observations, satellite estimates, and numerical model outputs, *Bull. Am. Meteorol. Soc.*, *78*, 2539-2558, 1997.

Xie, S.-P., A dynamic ocean-atmosphere model of the tropical Atlantic decadal variability, *J. Clim.*, *12*, 64-70, 1999.

Xie, S.-P., and S. G. Philander, A coupled ocean-atmosphere model of relevance to the ITCZ in the eastern Pacific, *Tellus*, *46A*, 340-350, 1994.

Xie, S.-P., and Y. Tanimoto, A pan-Atlantic decadal climate oscillation, *Geophys. Res. Lett.*, *25*, 2185-2188, 1998.

Zebiak, S. E., Air-sea interaction in the equatorial Atlantic region, *J. Clim.*, *6*, 1567-1586, 1993.

M. Barreiro, Program in Atmospheric and Oceanic Sciences, 205 Sayre Hall, Forrestal Campus, Princeton University, Princeton, NJ 08544-0710. (barreiro@princeton.edu)

P. Chang, Department of Oceanography, Texas A&M University, College Station, TX 77843-3146. (ping@tamu.edu)

A. Giannini, International Research Institute for Climate Prediction, Columbia University, Palisades, NY 10964-8000. (alesall@iri.columbia.edu)

R. Saravanan, National Center for Atmospheric Research, Boulder, CO 80307-3000. (svn@ncar.ucar.edu)

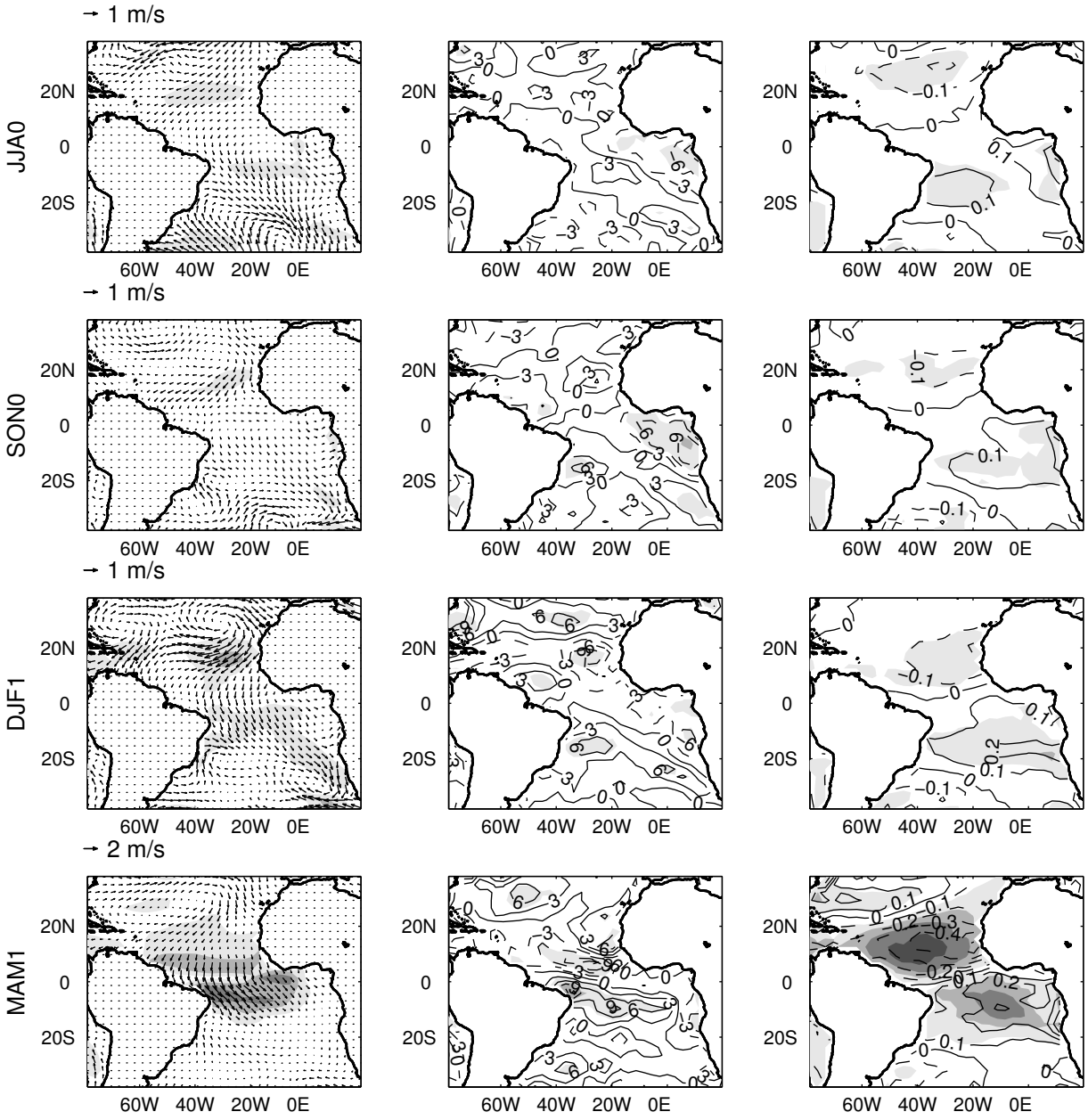

Figure 1. Lag-regression of 1000 hPa winds (left panels), surface downward heat flux (middle panels) and SST (right panels) anomaly onto the GI for seasons JJA0, SON0, DJF1 and MAM1. The GI index is constructed in MAM1. The regions used to construct the index are shown as boxes in the lower right panel. Arrows indicate the scale of 1000 hPa winds. The contour interval for heat flux is 3 W m^{-2}, and for SST is 0.1 K. Shading indicates the percentage of variance explained in intervals of 10%, 30%, 50%, and 70%. Explained variance of 10% is slightly above the 95% significance level. For surface winds the shading indicates explained variance in wind speed.

Figure 1. Lag-regression of 1000 hPa winds (left panels), surface downward heat flux (middle panels) and SST (right panels) anomaly onto the GI for seasons JJA0, SON0, DJF1 and MAM1. The GI index is constructed in MAM1. The regions used to construct the index are shown as boxes in the lower right panel. Arrows indicate the scale of 1000 hPa winds. The contour interval for heat flux is 3 W m^{-2}, and for SST is 0.1 K. Shading indicates the percentage of variance explained in intervals of 10%, 30%, 50%, and 70%. Explained variance of 10% is slightly above the 95% significance level. For surface winds the shading indicates explained variance in wind speed.

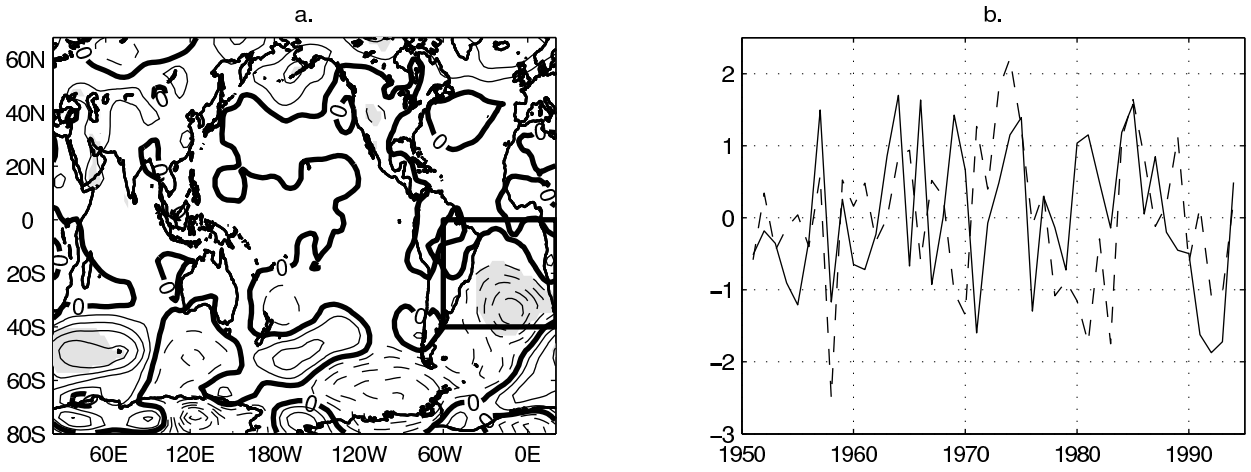

Figure 2. (a) Regression of sea level pressure onto the PC time series (P1JJAS) of winter-EOF during JJAS season. Spatial pattern of the leading mode of observed sea level The box marks the region in which the EOF analysis of 1000 hPa wind speed was performed. Contour interval is 20 Pa, and shading indicates significance at the 95% level. (b) Index P1JJAS (solid line) and GI time series (dashed line). P1JJAS is shifted 1-year so that it can be compared with GI index.

Figure 2. (a) Regression of sea level pressure onto the PC time series (P1JJAS) of winter-EOF during JJAS season. Spatial pattern of the leading mode of observed sea level The box marks the region in which the EOF analysis of 1000 hPa wind speed was performed. Contour interval is 20 Pa, and shading indicates significance at the 95% level. (b) Index P1JJAS (solid line) and GI time series (dashed line). P1JJAS is shifted 1-year so that it can be compared with GI index.

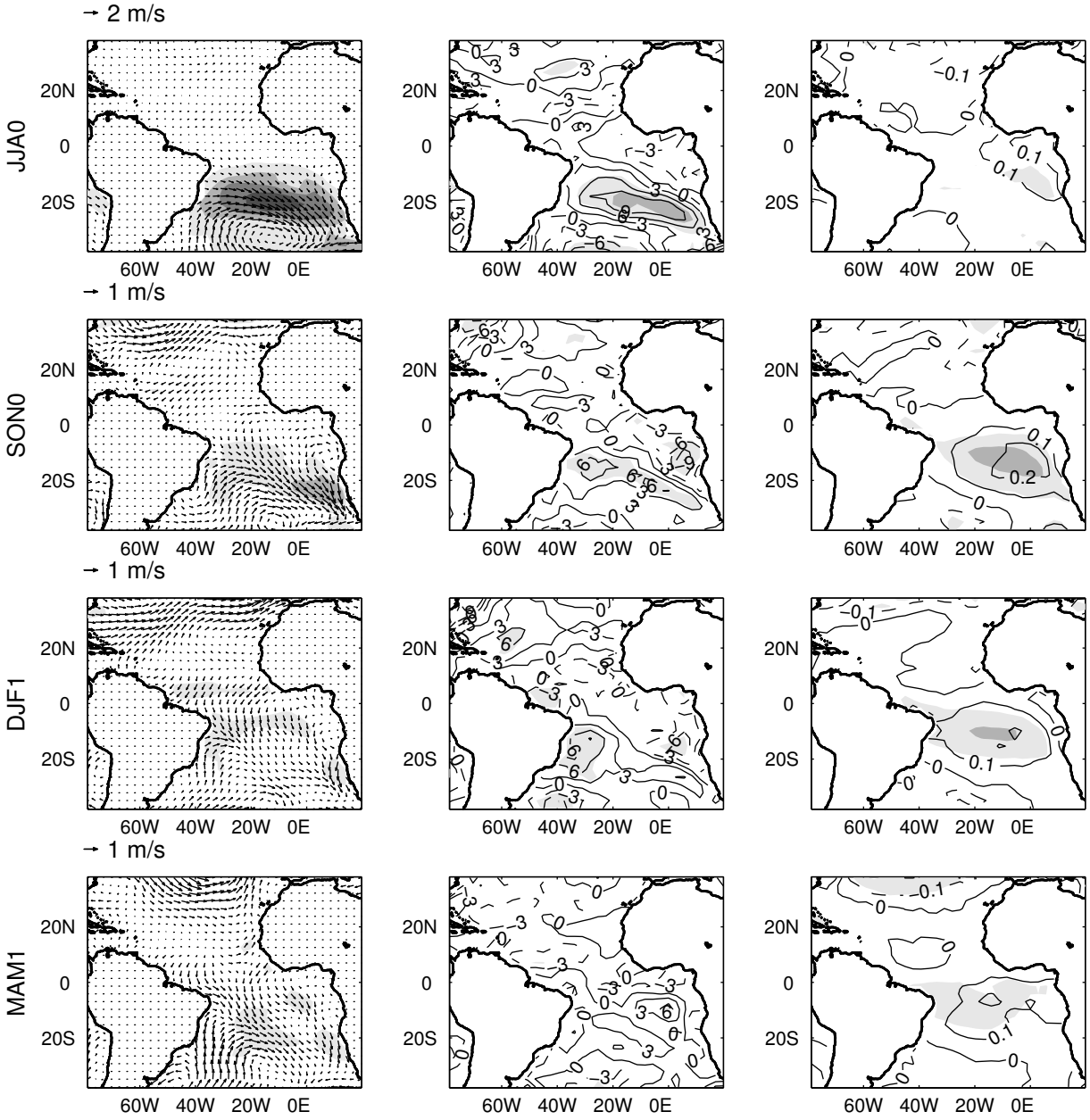

Figure 3. Same as Figure 1, but regressing onto the PC time series of the winter-EOF (P1JJAS) calculated in JJAS0.

Figure 3. Same as Figure 1, but regressing onto the PC time series of the winter-EOF (P1JJAS) calculated in JJAS0.

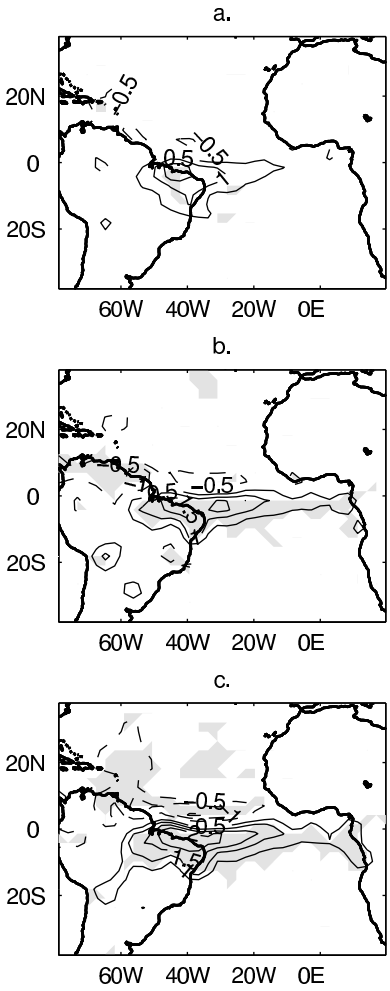

Figure 4. Regression of rainfall anomaly during MAM onto (a) P1JJAS, (b) P1NDJF, and (c) GI indices. The regression is performed during the period of 1979 to 1994. Shading indicates statistical significance at the 95% level. Contour interval is 0.5 mm day^{-1}.

Figure 4. Regression of rainfall anomaly during MAM onto (a) P1JJAS, (b) P1NDJF, and (c) GI indices. The regression is performed during the period of 1979 to 1994. Shading indicates statistical significance at the 95% level. Contour interval is 0.5 mm day^{-1}.

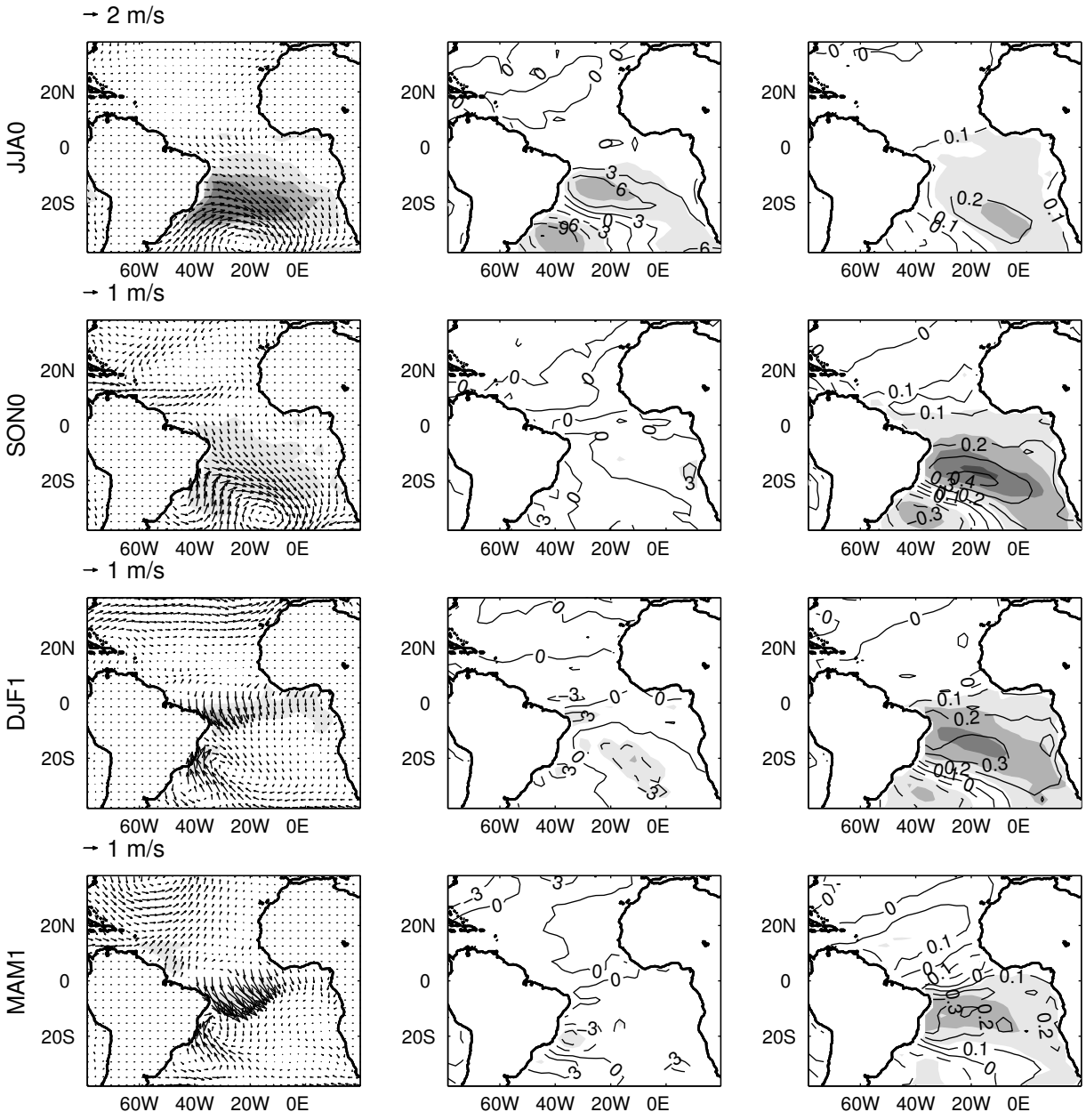

Figure 5. Same as Figure 3, but regressing onto the PC time series of the leading EOF of simulated wind-speed at 1000 hPa during JJAS0.

Figure 5. Same as Figure 3, but regressing onto the PC time series of the leading EOF of simulated wind-speed at 1000 hPa during JJAS0.

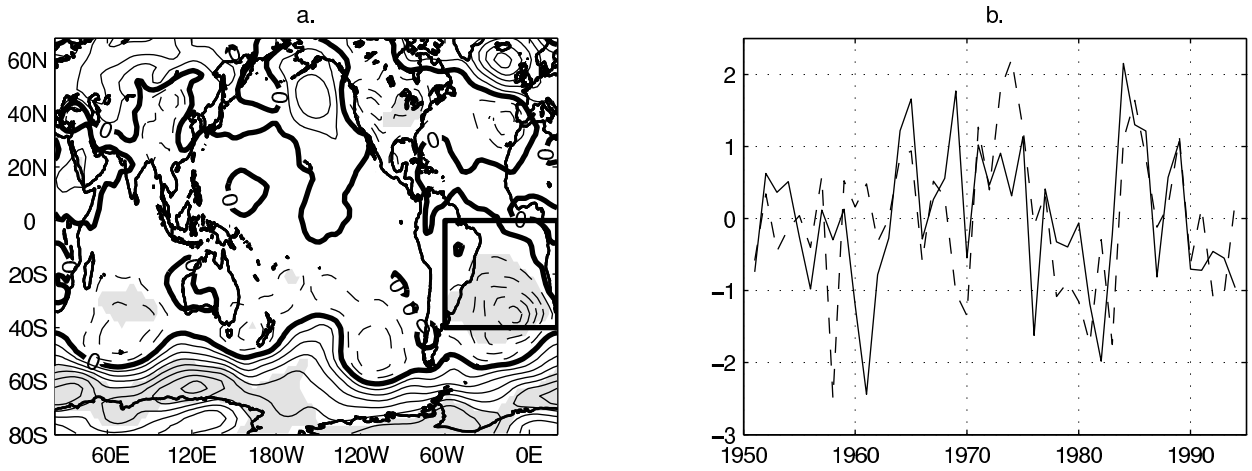

Figure 6. Same as Figure 2, but for the summer-EOF.

Figure 6. Same as Figure 2, but for the summer-EOF.

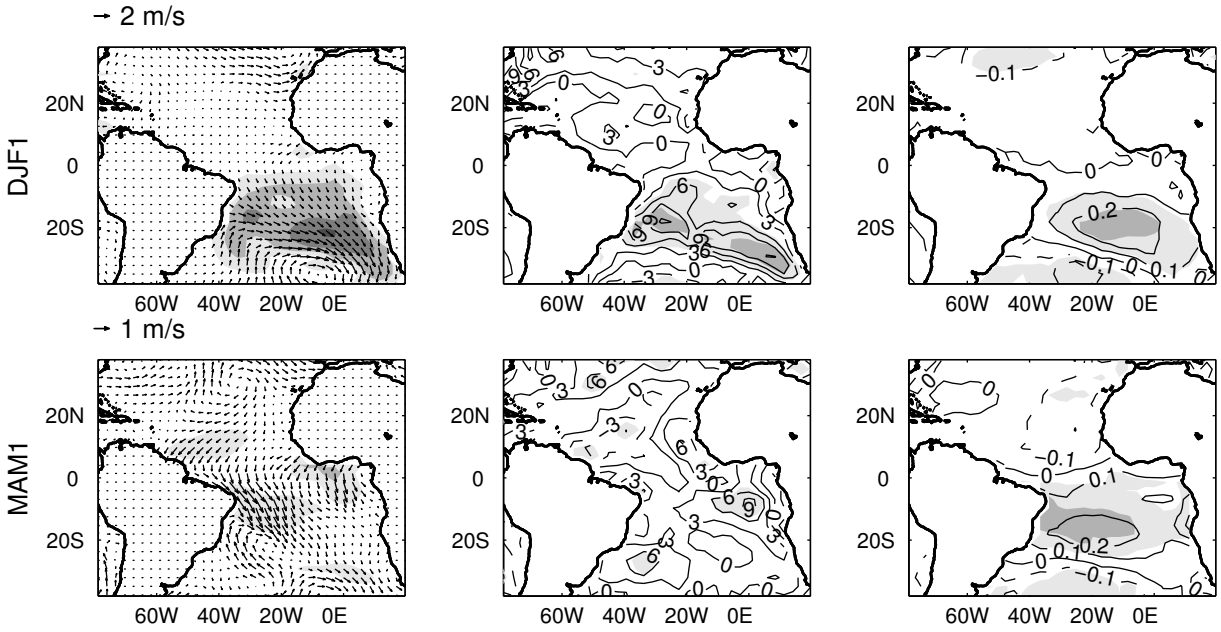

Figure 7. Lag-regression of 1000 hPa winds (left panels), surface downward heat flux (middle panels) and SST (right panels) anomaly onto the PC time series of summer-EOF (P1NDJF) for seasons DJF1 and MAM1. The P1NDJF index is constructed in NDJF1. Arrows indicate the scale of 1000 hPa winds. The contour interval for heat flux is 3 W m^{-2}, and for SST is 0.1 K. Shading indicates the percentage of variance explained in intervals of 10%, 30%, 50%, and 70%. Explained variance of 10% is slightly above the 95% significance level. For surface winds the shading indicates explained variance in wind speed.

Figure 7. Lag-regression of 1000 hPa winds (left panels), surface downward heat flux (middle panels) and SST (right panels) anomaly onto the PC time series of summer-EOF (P1NDJF) for seasons DJF1 and MAM1. The P1NDJF index is constructed in NDJF1. Arrows indicate the scale of 1000 hPa winds. The contour interval for heat flux is 3 W m^{-2}, and for SST is 0.1 K. Shading indicates the percentage of variance explained in intervals of 10%, 30%, 50%, and 70%. Explained variance of 10% is slightly above the 95% significance level. For surface winds the shading indicates explained variance in wind speed.

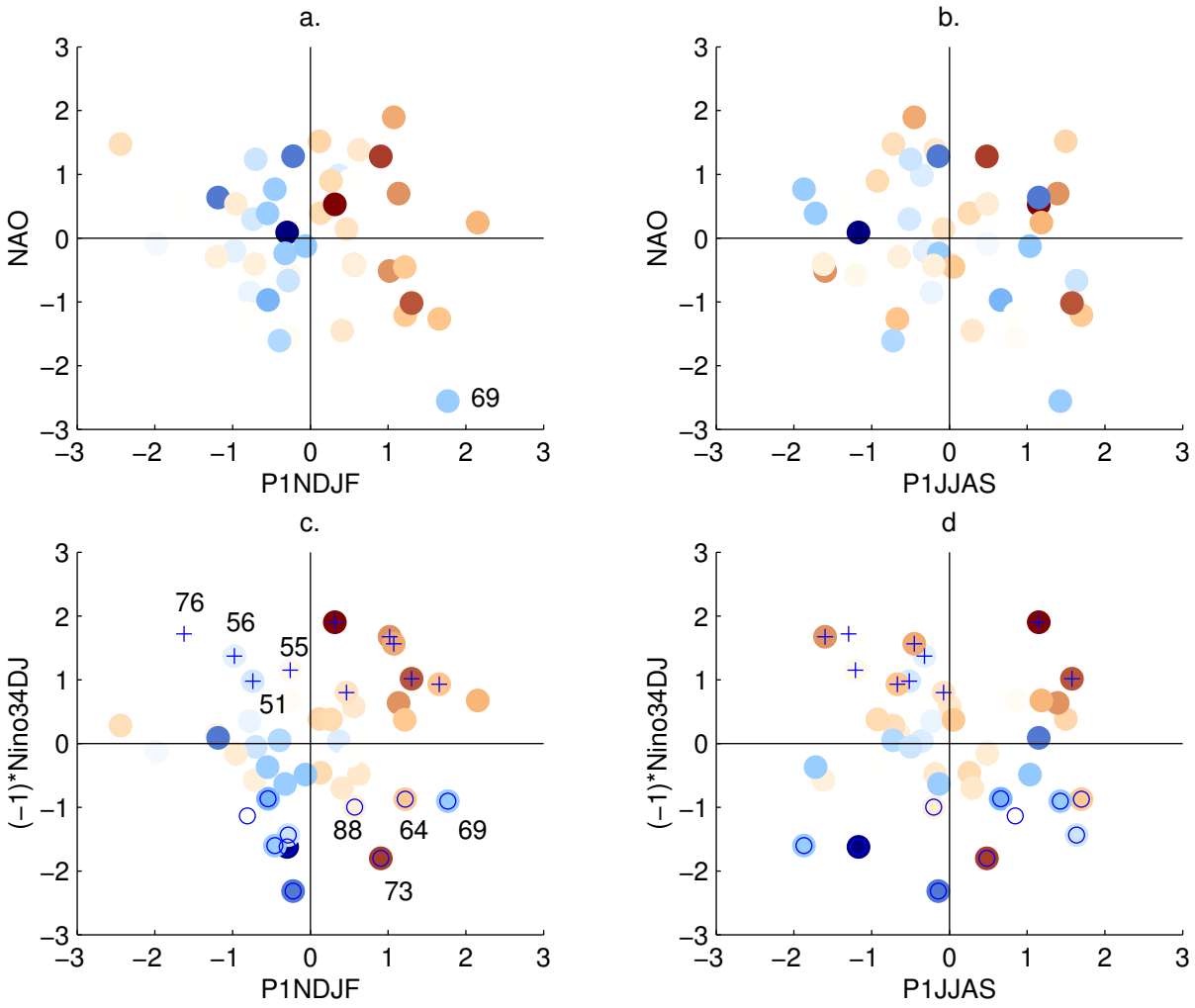

Plate 1. Scatter plots using as coordinates (a) P1NDJF and NAO, (b) P1JJAS and NAO, (c) P1NDJF and (-1)*Nino34DJ, and (d) P1JJAS and (-1)*Nino34DJ. In all plots the color of the markers indicates the intensity and sign of the GI: blue is negative, red is positive. In (c) and (d) "o" indicate El Niño years, and "+" indicate La Niña years. Specific ENSO events discussed in the text are identified by their years. Indices are normalized.

Plate 1. Scatter plots using as coordinates (a) P1NDJF and NAO, (b) P1JJAS and NAO, (c) P1NDJF and (-1)*Nino34DJ, and (d) P1JJAS and (-1)*Nino34DJ. In all plots the color of the markers indicates the intensity and sign of the GI: blue is negative, red is positive. In (c) and (d) "o" indicate El Niño years, and "+" indicate La Niña years. Specific ENSO events discussed in the text are identified by their years. Indices are normalized.